

# Application of platelet-rich plasma (PRP) improves self-renewal of human spermatogonial stem cells in two-dimensional and three-dimensional culture systems

Farnaz Khadivi<sup>a</sup>, Morteza Koruji<sup>b</sup>, Mohammad Akbari<sup>a</sup>, Ayob Jabari<sup>c</sup>, Ali Talebi<sup>d</sup>, Sepideh Ashouri Movassagh<sup>e</sup>, Amin Panahi Boroujeni<sup>f</sup>, Narjes Feizollahi<sup>a</sup>, Aghbibi Nikmahzar<sup>a</sup>, Mohammad Pourahmadi<sup>g</sup>, Mehdi Abbasi<sup>a,\*</sup>

<sup>a</sup> Department of Anatomy, School of Medicine, Tehran University of Medical Sciences, Tehran, Iran

<sup>b</sup> Stem Cell and Regenerative Medicine Research Center & Department of Anatomy, Iran University of Medical Sciences, Tehran, Iran

<sup>c</sup> Department of Obstetrics and Gynecology, Mollud infertility center, Zahedan University of Medical Sciences, Zahedan, Iran

<sup>d</sup> School of Medicine, Shahroud University of Medical Sciences, Shahroud, Iran

<sup>e</sup> Human and Animal Cell Bank, Iranian Biological Resource Center (IBRC), ACECR, Tehran, Iran

<sup>f</sup> Department of Anesthesiology, Shahrekord University of Medical Sciences, Shahrekord, Iran

<sup>g</sup> Department of Anatomy, Jahrom University of Medical Sciences, Jahrom, Iran

## ARTICLE INFO

### Keywords:

Human spermatogonial stem cells  
Self-renewal  
Platelet rich plasma  
Three dimensional culture system  
Growth factors  
Two dimensional culture system

## ABSTRACT

Spermatogonial stem cells (SSCs) are very sensitive to chemotherapy and radiotherapy, so male infertility is a great challenge for prepubertal cancer survivors. Cryoconservation of testicular cells before cancer treatment can preserve SSCs from treatment side effects. Different two-dimensional (2D) and three-dimensional (3D) culture systems of SSCs have been used in many species as a useful technique to in vitro spermatogenesis. We evaluated the proliferation of SSCs in 2D and 3D culture systems of platelet-rich plasma (PRP). Testicular cells of four brain-dead patients cultivated in 2D pre-culture system, characterization of SSCs performed by RT-PCR, flow cytometry, immunocytochemistry and their functionality assessed by xenotransplantation to azoospermia mice. PRP prepared and dosimetry carried out to determine the optimized dose of PRP. After preparation of PRP scaffold, cytotoxic and histological evaluation performed and SSCs cultivated into three groups: control, 2D culture by optimized dose of PRP and PRP scaffold. The diameter and number of colonies measured and relative expression of GFRA1 and c-KIT evaluated by real-time PCR.

Results indicated the expression of PLZF, VASA, OCT4, GFRA1 and vimentin in colonies after 2D pre-culture, xenotransplantation demonstrated proliferated SSCs have proper functionality to homing in mouse testes. The relative expression of c-KIT showed a significant increase as compared to the control group (\*:  $p < 0.05$ ) in PRP-2D group, expression of GFRA1 and c-KIT in PRP scaffold group revealed a significant increase as compared to other groups (\*\*\*:  $p < 0.001$ ). The number and diameter of colonies in the PRP-2D group showed a considerable increase ( $p < 0.01$ ) as compared to the control group. In PRP-scaffold group, a significant increase ( $p < 0.01$ ) was seen only in the number of colonies related to the control group.

Our results suggested that PRP scaffold can reconstruct a suitable structure to the in vitro proliferation of SSCs.

## 1. Introduction

According to the American Cancer Society, the annual incidence rate of childhood tumors aged birth to 19 years old is 186.6 per 1 million adolescents (Ward et al., 2014). Regarding the improvement in life expectancy through the efficient medical procedures, side effects of

treatment such as life quality and infertility are of grown importance (van Dorp et al., 2012). Spermatogonia are very sensitive to chemotherapy and radiotherapy, so male infertility is prevalent among survivors of childhood malignancy (Romerius et al., 2011). Because spermatogenesis does not begin up to pubescence, cryoconservation of a testicular tissue in prepubertal patients before cytotoxic therapies has

\* Corresponding author.

E-mail address: [abbasima@tums.ac.ir](mailto:abbasima@tums.ac.ir) (M. Abbasi).

<https://doi.org/10.1016/j.acthis.2020.151627>

Received 20 June 2020; Received in revised form 17 August 2020; Accepted 14 September 2020

Available online 28 September 2020

0065-1281/© 2020 Elsevier GmbH. All rights reserved.

been recommended (Nickholgh et al., 2014). It has been estimated the percentage of undifferentiated spermatogonia in mice and human are about 0.3 % and 22 % of germ cells, respectively. This limited amount of SSCs necessitates the in vitro proliferation and enrichment of SSCs (Fayomi and Orwig, 2018).

The microenvironment or niche of spermatogonial stem cells (SSCs) has critical roles in self-renewing and differentiation of SSCs in seminiferous tubules (Kostereva and Hofmann, 2008). In conventional 2D culture systems, the dishes are covered by collagen, matrigel, gelatin and other materials. While physical support for SSCs, microstructure and spatial pattern of the in situ seminiferous tubules provided by three-dimensional (3D) culture systems. 3D culture systems expanded our knowledge of the interactions between somatic cells and germ cells, extracellular matrix and germ cells, as well as the influence of interactions in the spermatogenesis. Artificially formed 3D constructions such as collagen gels (Lee et al., 2006), calcium cross-linked alginate molecules (Chu et al., 2009), soft agar culture system (Elhija et al., 2012) and methylcellulose culture system (Stukenborg et al., 2009) increased the proliferation of testicular cells, also directed the differentiation of SSCs. These findings recommending that viability, gene expression, cell morphology and differentiation of germ cells efficiently supported by communications in 3D culture systems. 3D culture condition organized cells into densely arranged clusters and provided useful structures which probably promoted the transfer of nutrients, oxygen, and growth factors that are crucial for clonal expansion and differentiation of SSCs (Huleihel et al., 2015). PRP clinically utilized from the 1970s as its tissue healing features, that is associated with its great level of secretory proteins and growth factors (Mei-Dan et al., 2011). Diverse growth factors including transforming growth factor b1 (TGF-b1), vascular endothelial growth factor (VEGF), platelet-derived growth factor (PDGF) and fibroblast growth factor (FGF), released from the a-granules of platelets after PRP activation (Eom et al., 2014). These factors stimulated a series of responses such as cell proliferation and cryoprotection, chemotaxis, production of collagen, angiogenesis, cellular migration and differentiation (Salamanna et al., 2015). The molecular mechanism of PDGF and its receptors was demonstrated on its ability to regulate the development of testis (Basciani et al., 2002). The mitochondrial cytochrome c/caspase pathway regulated by IGF-1, this signaling pathway increased cell proliferation (Li et al., 2003). IGF-1 significantly decreased sperm DNA damage (Susilowati et al., 2015). VEGF was found to activation of the nuclear factor erythroid 2-related factor 2 (Nrf2) pathway and consequently inhibited oxidative stress during spermatogenesis (Nakamura et al., 2010). Anti-inflammatory features of TGF-b led to a significant increase in concentration and motility of sperm (Sharkey et al., 2016). Activation of PRP by CaCl<sub>2</sub> solidified the plasma and forming the fibrin network. Fibronectin, fibrin and other proteins founded in PRP, act as adhesion molecules that can promote cell migration and fibrin network structure within the PRP can hold cells in a 3D organization. Consequently, Cell-PRP interaction may enhance stemness and increase the cell survival rate (Tobita et al., 2015). Since there is no available data on the proliferative effect of PRP on SSCs, this research focused on the self-renewing of adult human SSCs in two-dimensional and three-dimensional culture systems of PRP.

## 2. Materials & methods

### 2.1. Preparation of human testicular tissues

Human testes samples taken from four brain-dead donors at 17, 21, 25, and 26 years old from November 2018 to September 2019. Approval from the family of each donor was acquired by the Organ Procurement Unit (OPU) of Imam Khomeini Hospital affiliated to Tehran University of Medical Science for donate of the patient testes in a research protocol after necessary consent, the Ethics Committee of the Tehran University of Medical science (IR.TUMS.VCR. REC.1397.1125) authorized this research. Testicular samples used in this research revealed normal

spermatogenesis as proven by histology (data not shown) and Patients had no history of cancer chemotherapy or radiotherapy. The samples were placed in tissue bag containing phosphate-buffered saline (PBS; Gibco, Life Technologies, Grand Island, NY, USA) and 100 U/mL pen/strep (Gibco, Life Technologies, Grand Island, NY, USA). The samples were conveyed to the cell culture laboratory of Tehran University of Medical Sciences, washed three times with PBS, tunica albuginea removed and divided mechanically into small pieces.

### 2.2. Human testicular cells isolation

Isolation of testicular cells done according to the previously described protocol (Mirzapour et al., 2017), using two steps of enzymatic digestion protocol. Summarily, the fragmented testicular tissues transferred to the sterile 15 mL conical tube including first digestion mixture (Dulbecco modified Eagle medium (DMEM; Gibco, Life Technologies, Grand Island, NY, USA) supplemented by pen/strep, 1 mg/mL collagenase type I (Gibco, Life Technologies, Grand Island, NY, USA), 1 mg/mL trypsin, 0.05 mg/mL DNase and 1 mg/mL hyaluronidase (all from Sigma-Aldrich St. Louis, MO, USA)). After that, conical tube placed in a shaker incubator at 37 °C with 150 cycles per minute for 40 min, centrifuged for 4 min at 1100 rpm and cell plate washed with DMEM medium. For the second digestion step, cell plate obtained from the first enzymatic digestion suspended in another sterile 15 mL conical tube comprising the second digestion mixture. The second digestion protocol similar to the first digestion performed for 30 min. Collected cells filtered by a 40 µm nylon filter and washed three times by PBS supplemented by 100U/mL pen/strep. A hemocytometer was used to calculate the number of obtained cells and cell viability investigated by 0.04 % Trypan blue (Sigma-Aldrich St. Louis, MO, USA). Differential planting is a widely-used procedure for the separation of germ cells from somatic cells because Sertoli cells adhere to the culture plate quicker than SSCs. Isolated testicular cells were incubated overnight in uncoated plates with DMEM/F-12 (Gibco, Life Technologies, Grand Island, NY, USA) supplemented by 10 % fetal bovine serum (FBS; Gibco, Paisley, Uk), 100 U/mL pen/strep at 35 °C, nonattached cells were centrifuged at 1000 rpm for 5 min and cultured on the new uncoated flasks.

### 2.3. 2D pre-culture and proliferation of testicular cells

The floating cells obtained from differential plating method were cultured for 3 weeks in the basic culture medium including DMEM/F-12 medium supplemented by 100 IU/mL pen/strep, 40 µg/mL gentamycin (Invitrogen, Carlsbad, CA, USA), 20 ng/mL glial-derived nerve growth factor (GDNF; G1777, Sigma-Aldrich St. Louis, MO, USA), 10 ng/mL basic fibroblast growth factor (bFGF; F0291, Sigma-Aldrich St. Louis, MO, USA), 10 ng/mL leukemia inhibitory factor (LIF; L5283, Sigma-Aldrich St. Louis, MO, USA), 5% FBS, 5% knock-out serum replacement (KSR; Invitrogen, Carlsbad, CA, USA) and then maintained at 35 °C in a humidified atmosphere with 5% CO<sub>2</sub>, the medium replaced every 2 days. Cells were passaged with Trypsin-EDTA 0.25 % (25200; Invitrogen, Carlsbad, CA, USA) in several new uncoated flasks when they became 80 %–90 % confluent. The proliferation of Sertoli cells and formation of SSCs colonies was assessed by an inverted microscope (Zeiss, Jena, Germany), the cultured cells harvested for further characterization after the third week.

### 2.4. Confirmation of SSCs

#### 2.4.1. RT-PCR analysis

To prove the existence of SSCs in our experimental groups, the expression of human SSCs genes such as VASA, OCT4, PLZF and the Sertoli cells specific gene including Vimentin assessed after two steps of enzymatic digestion and after the 2D pre-culture of testicular cells were evaluated by RT-PCR, all evaluations were performed in three replications. Total RNA extracted according to the manufacturer's

recommendations using qiazol reagent (Qiagen, Hilden, Germany) from samples. Isolated RNA concentration evaluated by utilizing spectrophotometry (Eppendorf, Hamburg, Germany). To eradicate the contamination of genomic DNA, DNase I treatment (Fermentas, Waltham, MA, USA) performed. cDNA synthesis made by using 1 µg of isolated RNA, oligo (dT), random hexamers and first-strand cDNA synthesis kit (Fermentas, Waltham, MA, USA) according to the manufacturer's protocols. In Table 1, the sequences of primers are shown. The PCR cycles were set as denaturation stage at 95 °C for 30 s, annealing stage at 59–70 °C for 45 s, extension stage at 72 °C for 45 s, final polymerization at 72 °C for 10 min. The PCR products exposed to 1.5 % (w/v) agarose gel electrophoresis containing ethidium bromide (10 µg/mL). Eventually, gels were visualized by gel documentation system, with UV Transilluminator.

#### 2.4.2. Flow cytometry

The purification rate of SSCs evaluated by flow cytometrical analysis using the PLZF marker, this is one of the most appropriate markers for the undifferentiated SSCs isolation. Flow cytometry technique performed after two steps of enzymatic digestion and after the 2D pre-culture and more than 10<sup>5</sup> cells were used in each run. Briefly, after fixation with 4% paraformaldehyde (PFA, Merck KGaA, Darmstadt, Germany), 0.4 % Triton X100 (Sigma-Aldrich St. Louis, MO, USA) were used for permeabilization. After that, 10 µl of primary antibody (mouse monoclonal anti-PLZF antibody, 1:100, ab104854, Abcam, Cambridge, MA, USA) added to the approximately 10<sup>6</sup> cells at room temperature overnight. After twice washing with PBS, anti-mouse secondary antibody conjugated with FITC (1:200; ab97022, Abcam, Cambridge, MA, USA) was added at 4 °C, all experiments were performed in three replications. Stained cells evaluated by flow cytometry (Partec AG, CH-4144 Arlesheim, and Switzerland) equipped with a 15-mW argonion laser at an excitation wavelength of 488 nm and unstained cells (without primary antibody staining) considered as negative controls.

**Table 1**

The sequence of designed primers used for real-time PCR and RT-PCR analysis.

Gene name	Sequences	Product size (bp)	Annealing temperature (°C)
VASA	F:5'- ATCAACCCCTCATCTGTCTTCC-3'	196	60
	R:5'- TATTACTACTCACCACCATCTCT-3'		
OCT 4	F:5'- GGGGTGATACTTGAGTGAGAGA-3'	135	60
	R:5'- GGAGGTTGGAGTGAGCTGAGA-3'		
PLZF	F:5'- GTTGGAGTGAGATGAAGGAAGG-3'	262	60
	R:5'- AAGGTATGGGTGAAGGAAGGAGA-3'		
VIMENTIN	F:5'- TCAGAATATGAAGGAGGAAATG -3'	156	60
	R:5'- AGGGAGGAAAAGTTTGAAGAG -3'		
GAPDH	F:5'- CATGAGAAGTATGACAACAGCCT-3'	113	60
	R:5'- AGTCTTCCACGATACCAAAGT-3'		
GFRA1	F:5'- TTCAGCAAGTGAGCACATTTC-3'	141	60
	R:5'- GGTTGCAGACATCGTTGGAC-3'		
c-KIT	F:5'- AACACGCACCTGCTGAAATG-3'	179	60
	R:5'- GTCTACCACGGGCTTCTGTGC-3'		

#### 2.4.3. Xenotransplantation of human SSCs

Isolated human testicular cells after 2D pre-culture were transplanted into the seminiferous tubules of recipient immunodeficient male, National Medical Research Institute (NMRI), mice which were mature (n = 10; 6–8 weeks of age) weighing between 27.7 and 31.9 g to approve the attendance of functional SSCs in our experimental groups (Kubota and Brinster, 2018). Mature mice nurtured in the Razi laboratory of Tehran, Iran, kept to the Tehran University of Medical Sciences with suitable animal conditions (food and water ad libitum). All animal care and experimental procedures approved according to the rules presented by the Ethics Committee of Tehran University of Medical Sciences. To destroy the endogenous spermatogenesis, the recipient mice were given intraperitoneally single dose 40 mg/kg of busulfan (Sigma-Aldrich, Deisenhofen, Germany) 8 weeks before donor cell transplantation. The cultured cells were labeled with DiI (Invitrogen, Cergy Pontoise, France) according to the manufacturer's protocol. The recipient mice were deeply anesthetized with an intraperitoneal injection of ketamine and xylazine (with the ratio of 10/1) (Serva Feinbiochemica, Heidelberg, Germany). Transplantation was done through retrograde injection into the ductus efferentes. Approximately, 10<sup>5</sup> cells from the 2D pre-cultured in 10 µl DMEM injected into the left seminiferous tubules of every recipient mouse and right testis considered as internal control. Nearly, 70–80 % of the seminiferous tubules visualized and followed by exerting trypan blue in the injection media of spermatogonial cells. The mice were sacrificed 8 weeks after transplantation, both testes were removed and fixed in 10 % neutral-buffered formalin. To assess the presence of DiI-labeled SSCs, the serial-sections from left testis were obtained. Finally, sections were counterstained with 4, 6-diamidino-2-phenylindole (DAPI; 1 µg/mL; Sigma-Aldrich St. Louis, MO, USA) to prove the results. The presence and proliferation of injected cells investigated through fluorescent microscope (Olympus BX51TRF, Tokyo, Japan) and equipped with a digital camera (Nikon, 191 Tokyo, Japan).

#### 2.4.4. Characterization of SSCs colonies by immunocytochemistry

To identification of human SSCs colonies after 2D pre-culture for three weeks, expression of PLZF and GFRA1 assessed by immunocytochemistry. Human testicular cells cultured in 24-well culture plates, fixed with 4% PFA for 15 min at room temperature, permeabilized with 0.5 % Triton X-100 for 30 min. Nonspecific adhesion sites blocked with 10 % goat serum (Sigma-Aldrich St. Louis, MO, USA). The plates were incubated with primary antibodies (anti-PLZF antibody (D-9): sc-28319, a mouse monoclonal IgG1 PLZF antibody, 1:100, anti-GFR alpha-1 antibody (E-11): sc-271546, a mouse monoclonal IgG1 GFRα-1 antibody, 1:100) for 2 h at 37 °C (primary antibodies acquired from Santa Cruz Biotechnology). After washing with PBS, anti-mouse secondary antibody conjugated with FITC (1:200; ab97022, Abcam, Cambridge, MA, USA) was added for 3 h at room temperature. The primary antibody removed for control cells and nuclei counterstained with DAPI. Consequently, the fluorescent images were taken by a fluorescence microscope (Olympus BX51TRF, Tokyo, Japan) equipped to a digital camera (Nikon, 191 Tokyo, Japan).

#### 2.5. PRP preparation and dosimetry

PRP prepared by the Iran blood transfusion organization (Tehran, Iran) from the complete blood of healthy candidate. The PRP attained in a bag containing Citrate Phosphate Dextrose Adenine Solution (CPDA; C4431 Sigma-Aldrich St. Louis, MO, USA) as anti-coagulant. To remove erythrocytes entirely and minimize their interference, care was taken. The platelet count measured by an automatic counter (Sysmex, XS-800i, Kobe, Japan). Since no study has been done on the proliferation of SSCs in 2D culture system of PRP, the viability of testicular cells at different concentrations of PRP investigated by Methylthiazolyldiphenyl-tetrazolium bromide (MTT) (Sigma-Aldrich St. Louis, MO, USA) assay at days 3, 7 and 14 to determine the optimal dose of PRP.

Cells cultured by 4 different doses of PRP for 2 weeks:

- 1) Cells cultured in basic culture medium+ 1% PRP,
- 2) Cells cultured in basic culture medium+ 2.5 % PRP
- 3) Cells cultured in basic culture medium+ 5% PRP,
- 4) Cells cultured in basic culture medium+ 10 % PRP

On the third, seventh and fourteenth days, cells transferred into a 96-wells culture plate at a density of  $10^5$  cells per well and incubated in DMEM medium containing 0.05 mg/mL Methylthiazolyldiphenyl-tetrazolium bromide (MTT) for 4 h at 37 °C in a 5% CO<sub>2</sub> incubator, all experiments were carried out in five replications. After that, cells lysed and purple formazan crystals dissolved by adding 100 µl dimethyl sulfoxide (DMSO; 1.4 M; D8418 Sigma-Aldrich, Germany), per well for 30 min at room temperature. Finally, a microplate reader (EONTM, BioTek, USA) used to measure the optical density (OD) of each well at 570 nm wavelength.

## 2.6. Preparation of PRP scaffold and reconstitution of testicular cells on it

To make the PRP scaffold, we mixed PRP (obtained from the complete blood of healthy candidate by the Iran blood transfusion organization) with Calcium chloride (CaCl<sub>2</sub>; Catalog no: 102382, Merck KGaA, Germany) at a 9:1 ratio in 12-wells plates. The mixture was incubated at 37 °C and 5% CO<sub>2</sub> for 15 min to create the hydrogel (Xie et al., 2012). Due to the addition of CaCl<sub>2</sub>, a flexible fibrin scaffold formed within a few minutes. This bioactive structure applied for cell seeding and could be manipulated into different shapes. Then, cells ( $1.3 \times 10^6$ ) per 200 µl of culture medium (DMEM/F-12 medium containing 100 IU/mL pen-/strep, 40 µg/mL gentamycin, 20 ng/mL GDNF, 10 ng/mL bFGF, 10 ng/mL LIF, 5% FBS, 5% KSR) seeded in a 12-wells plate on PRP scaffold and incubated at 37 °C and 5% CO<sub>2</sub> for 4 weeks to perform further analysis.

### 2.6.1. Cytotoxicity analysis of PRP scaffold

The cytotoxicity of the PRP scaffolds evaluated by MTT colorimetric assay. PRP scaffolds (n = 5, each experiment was carried out in five replications) made at a 96-wells culture plate,  $10^5$  cells per well cultured on each scaffold and MTT assay were done 24 h and 48 h after cell seeding, according to the protocol mentioned above. To eliminate the probable formazan production by the platelets, MTT was also done for cells without PRP scaffolds as a blank.

### 2.6.2. Scanning electron microscopy (SEM)

SEM observations were performed for the evaluation of scaffold structure and SSCs colonies after cell culture. PRP scaffolds fixed with 2.5 % glutaraldehyde (Sigma-Aldrich St. Louis, MO, USA) at pH 7.4 for 2 h, dehydrated by increasing concentrations of ethanol for 15 min intervals. The dried specimens were then covered with gold sputter-coating and seen under an environmental scanning electron microscope (SEM, CamScan, MV2300, UK). SEM micrographs analyzed by the ImageJ software (ImageJ, free Java software provided by the National Institute of Health, Bethesda, Maryland, USA) for measuring the pores size of scaffold, the number and diameter of SSCs colonies in each field (Schindelin et al., 2015).

### 2.6.3. Histological evaluation of PRP scaffold

Hematoxylin/eosin (H& E) staining performed to verify the histological structure of the PRP scaffold and evaluating the SSCs colonies on the PRP scaffold after the first week.

Scaffolds primarily were fixed in 10 % neutral buffered formalin, dehydrated through increasing concentrations of ethanol, after clearing by xylene and embedding in paraffin wax, sectioned at a thickness of 5 µm. Sections deparaffinized, rehydrated, stained with H& E and mounted in entellan (all from Merck, Germany). Tissue analysis performed using light microscopy (Olympus CH30, Japan) (Khadivi et al.,

2020).

### 2.6.4. Biodegradation and hydration test

1 mL Trypsin-EDTA (25200; Invitrogen, Carlsbad, CA, USA) added to PRP-scaffolds (n = 5, five replications for biodegradation test) and incubated at 37 °C for 3 days. To prevent the loss of enzymatic activity, the trypsin substituted daily with a fresh solution. The PRP-scaffolds weighed before trypsin administration and at the end of the third day. The rate of enzymatic degradation measured by subtracting the start weight and end weight of the scaffolds.

To evaluation of hydration test, the water content measured. Water content calculated by subtracting overnight dried and freshly prepared scaffolds (n = 5, five replications for hydration test) weight.

## 2.7. Experimental design

SSCs cultured for four weeks at 3 groups including 1) control group (2D culture of SSCs in basic culture medium), 2) 2D culture of SSCs in basic culture medium and the selected dose of PRP, 3) 3D culture of SSCs on the PRP scaffold

Cell culture performed with  $10^6$  cells for each group on a 12-wells plate and further analysis done. According to the different groups, several small clusters were observed on top of the monolayer from testicular cells, approximately after 10 days.

## 2.8. Gene expression evaluation by quantitativeReal-time PCR

The relative expression levels of GFRA1, involved in the preservation of the undifferentiated state and c-KIT were assessed by real-time PCR, the specific primers are listed in Table 1. The RNA of the cells extracted by using the Trizol reagent kit (Ready Mini Kit, Qiagen, Hilden, Germany) and the manufacturer's instruction. The purity and concentration of RNA determined using ND-3800 spectrophotometer (Nano-drop Technologies, Hercules, Malaysia). Total RNA (2 µg) applied for cDNA using a Prime Script RT reagent kit (Takara Bio Inc, Tokyo, Japan) according to the manufacturer's protocols. Real-time PCR carried out in 40 reaction amplification cycles by a qPCR machine (Applied Biosystems, Foster City, USA) and the SYBR Premix Ex Taq Kit (Tli RNaseH Plus). Analysis of melting curve made after every run to identify the existence of primer dimers and nonspecific PCR products. As an internal control, all samples normalized against glyceraldehyde-3-phosphate dehydrogenase (GAPDH). The relative quantification of gene expression was investigated through the comparative CT method ( $\Delta\Delta CT$ ).

## 2.9. Cell proliferation and morphological evaluation of colonies

Four weeks after cell seeding, the viability and proliferation of SSCs at different groups evaluated by MTT assay. As well as, the number of colonies and the diameter of each colony determined at different groups. The inverted microscopic images (Zeiss, Jena, Germany) and SEM micrographs were used to define the number of colonies, experimental evaluations were carried out in five different fields and three replicates for each group. Image J software was applied to measure the diameter of each colony.

## 2.10. Statistical analysis

The SPSS (Version 22.0. IBM Corp, Armonk, New York) software was used for data analysis. All data expressed as mean  $\pm$  standard deviation of the mean (mean  $\pm$  SD); Kolmogorov-Smirnov test applied to determine the normal distribution of data, for multiple comparisons of data, One-Way ANOVA used. Statistical significance between control and experimental groups calculated by one-way analysis of variance (ANOVA) followed by Tukey's test.  $P \leq 0.05$  was considered statistically significant.

### 3. Results

#### 3.1. Isolation and identification of human SSCs and Sertoli cells by RT-PCR

The viability of freshly isolated cells after enzymatic digestion was more than 80 %, as evaluated by the dye exclusion test (0.04 % trypan blue solution) (data not shown).

RT-PCR performed to evaluate the expression of PLZF (spermatogonial specific marker), VASA (germ cell marker), OCT4 (stemness marker), and Vimentin (a marker for Sertoli cells) after two steps of enzymatic digestion and after the 2D pre-culture of testicular cells. All samples expressed PLZF, OCT4, VASA, and Vimentin. GAPDH was also used as a housekeeping gene. After 2D pre-culture of testicular cells a significant increase in expression of OCT4, Vimentin, and VASA observed in comparison to after digestion ( $p < 0.01$ ) (Fig. 1). No significant increase observed in the expression of PLZF after 2D pre-culture of testicular cells. Collectively, these data recommend that the isolated cells phenotypically are human SSCs.

#### 3.2. Evaluation of the purification of SSCs by flow cytometry

Flow cytometry analysis using the PLZF marker carried out on the supernatant after two steps of enzymatic digestion and after the 2D pre-culture to assess the purity of SSCs. Our results indicated that 16.2 % of all cells were positive for PLZF after enzymatic digestion (Fig. 2B). Whereas after the 2D pre-culture significantly increased the purity of SSCs to 80.2 % (Fig. 2D).

#### 3.3. Analysis of recipient mouse testes after xenotransplantation

In histological sections from the normal seminiferous tubules of mice, the intact arrangement of seminiferous tubules associated with the spermatogenic cells seen (Fig. 3A). Distortion and atrophy in the germinal epithelium, also reduction in the diameters and thickness of seminiferous tubules seen in Busulfan treated mice (Fig. 3B). Structural investigation of seminiferous tubules under the fluorescent microscope 8 weeks after xenotransplantation was done. The result indicated that labeled cells transplanted on the seminiferous tubules basement membrane in recipient testes as an individual cell and didn't create a cluster (Fig. 3C). This is a morphological distinction of undifferentiated spermatogonia that proved the existence of SSCs after 2D pre-culture and evaluate the homing and colonization of SSCs in the recipient testis. The non-transplanted right testis considered as the control group (Fig. 3D).

#### 3.4. Immunocytochemistry evaluation of colonies

Single-cell suspensions obtained after enzymatic digestion of human testicular tissues proliferated in basic culture medium for three weeks. As shown in Fig. 4, we identified the expression of PLZF and GFRA1 by immunocytochemistry on human SSCs colonies.

#### 3.5. PRP dose selection

To determine the optimized dose of PRP for SSCs culture, we performed MTT assay at 4 different doses of PRP on the third, seventh and fourteenth days. Higher viability and proliferation of SSCs observed at culture medium with 5% PRP (Fig. 5). When we used 10 % PRP, we interestingly observed greater colonies that exhibited the appearance of human embryonic stem cell-like colonies. The germ line stem cell colonies introduced as an aggregation of individually obvious cells while the embryonic stem cell-like cells colonies were compact and sharply edged.

#### 3.6. Cytotoxic evaluation of PRP scaffold

We used MTT assay to assess cell viability on the PRP scaffold in the first and second days after cell seeding (Fig. 6). The proliferation rate and viability of the SSCs on PRP scaffolds showed a striking time-dependent increase ( $***: p < 0.001$ ), ( $** : p < 0.01$ ) as compared to only PRP- scaffold.

#### 3.7. Components and physical properties of PRP scaffold

According to the SOP of the Iran blood transfusion organization, every plasma bag should contain at least  $55 \times 10^9$  platelets. The average PRP platelet count was  $638 \times 10^3$  platelets/ $\mu$ l. SEM images obtained from the PRP scaffold exhibited the porous structure (Fig. 7A), the results of image j analysis indicated the mean of pores size was  $46.87 \pm 6.77$ , and the content of water (gr) after overnight incubation was  $4.738 \pm 1.15$ . Degeneration of scaffolds after 3 days and following the application of trypsin was  $0.706 \pm 0.23$ . After the formation of the PRP scaffold by calcium chloride, PRP commenced cross-linking and slowly made a clear, elastic hydrogel. The fresh PRP scaffolds were semi-transparent, light yellowish, easy to slicing and could be exerted in different shapes. Histological sections from PRP scaffolds stained by H&E revealed cross-linked fibrin in pink (Fig. 7B) these randomly oriented fibrils organizations appeared to present an efficient microstructure for human SSCs to adhere and colonization.

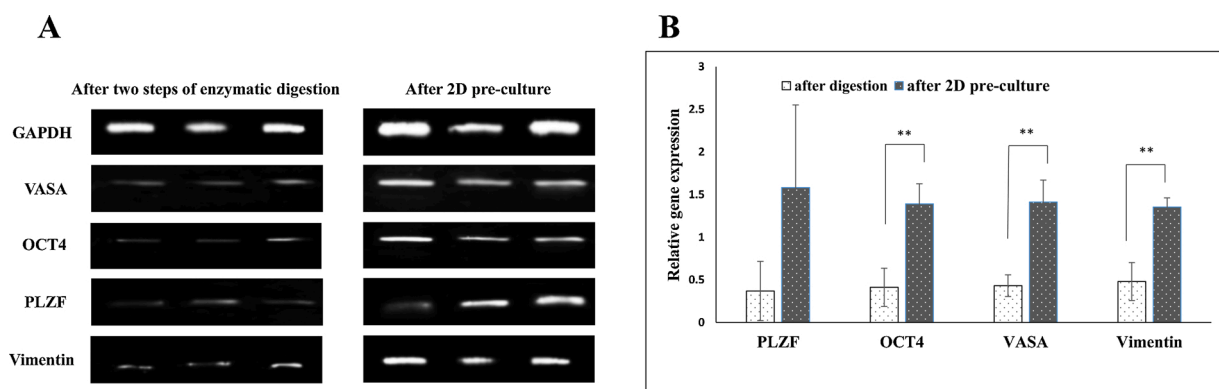


**Fig. 1.** Molecular definition of SSCs and Sertoli cells at the RNA level by RT-PCR. A) RT-PCR was utilized to determine the expression of specific spermatogonia and Sertoli cell markers in isolated testicular cells after two steps of enzymatic digestion and after 2D pre-culture. GAPDH was also applied as a housekeeping gene and all evaluations were performed in three replications. B) Expression of the spermatogonia and Sertoli cells specific genes including VASA, OCT4, and Vimentin increased significantly after the 2D pre-culture of SSCs, values expressed as means  $\pm$  SD (\*\*:  $p < 0.01$ ) in comparison to after two steps of enzymatic digestion.

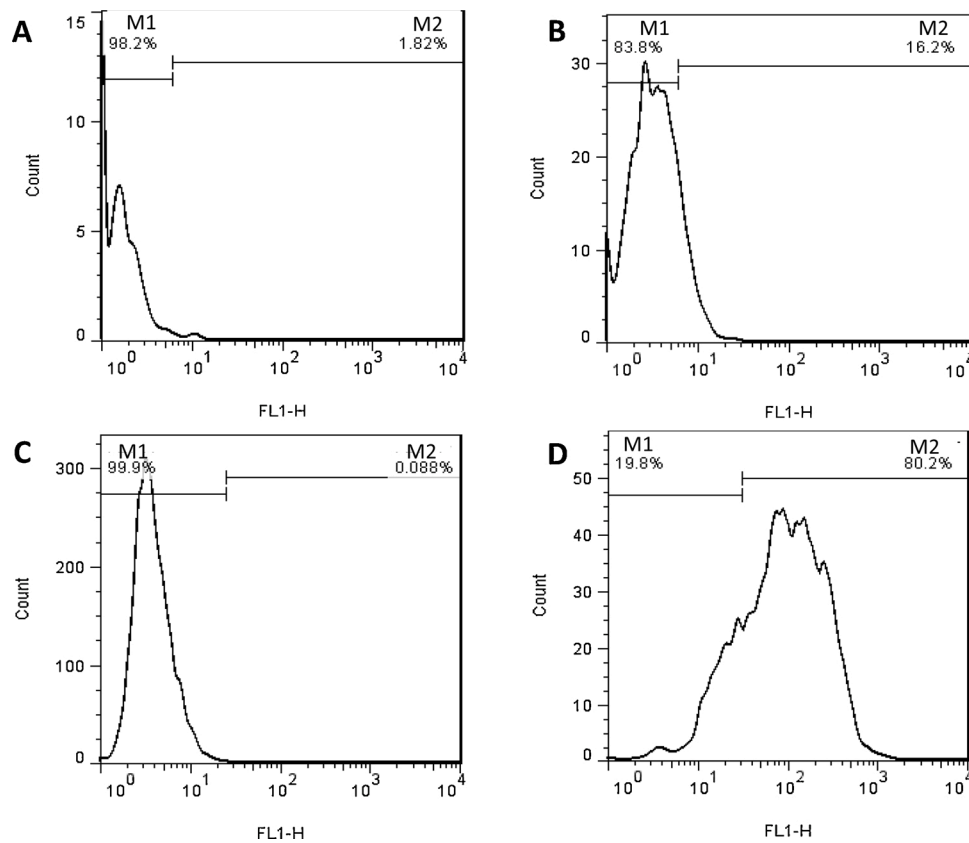


**Fig. 2.** Flow cytometry identified the SSCs purity percentage with PLZF marker, approximately  $10^6$  cells were utilized for each measurement. A, B) after two steps of enzymatic digestion, C, D) after the 2D pre-culture, data were analyzed and presented by Flowjo software. A and C are control cells that primary antibody was eliminated. M1: PLZF-negative cells, M2: PLZF-positive cells.

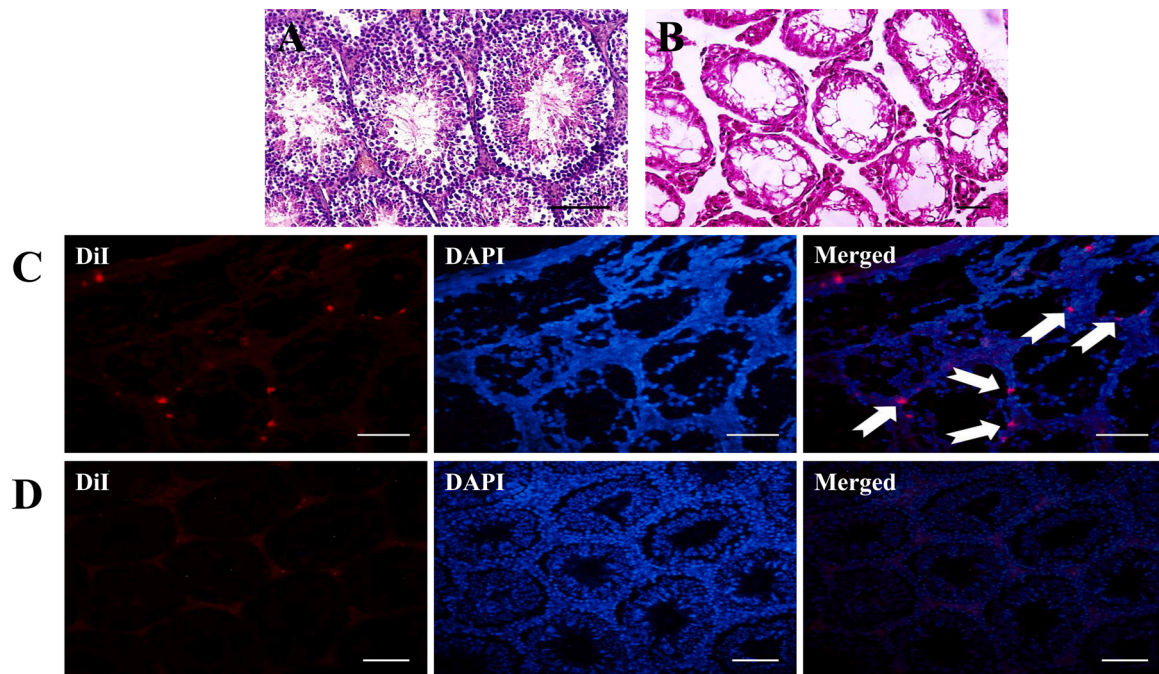


**Fig. 3.** A) The sections obtained from the normal seminiferous tubules of mice stained by H&E displayed by light microscopic images, the normal organization of germ cells and the regular architecture of the seminiferous tubules can be recognized. B) The sections of seminiferous tubules in the busulfan treated mice stained by H&E, morphological disorders in the germinal epithelium of seminiferous tubules such as atrophy and disorganization seen, the thickness of the germinal epithelium and the number of spermatogenic cells significantly decreased. C) Fluorescent microscopic images exhibited the sections of seminiferous tubules in recipient infertile mice 8 weeks after xenotransplantation, human SSCs labeled with DiI transplanted on the basement membrane of the seminiferous tubules, D) Non-transplanted testis was regarded as the control group, in order to confirm the results DAPI nucleus staining performed (C, D). Scale bars = 200  $\mu$ m.

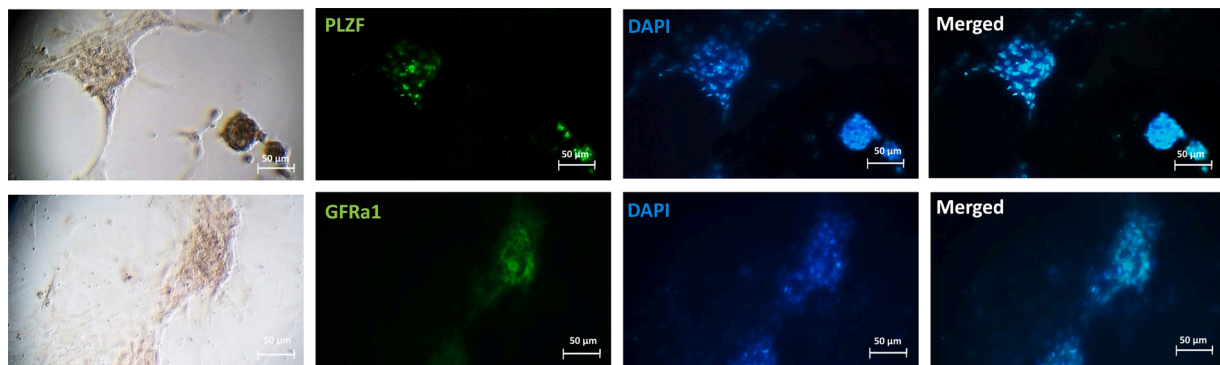


**Fig. 4.** Immunofluorescent staining of SSCs colonies. Fluorescent microscopic images of human SSCs colonies after 2D pre-culture for 3 weeks displayed SSCs were positive for PLZF and GFRa1, nuclei counterstained with DAPI (blue) (For interpretation of the references to colour in this figure legend, the reader is referred to the web version of this article).

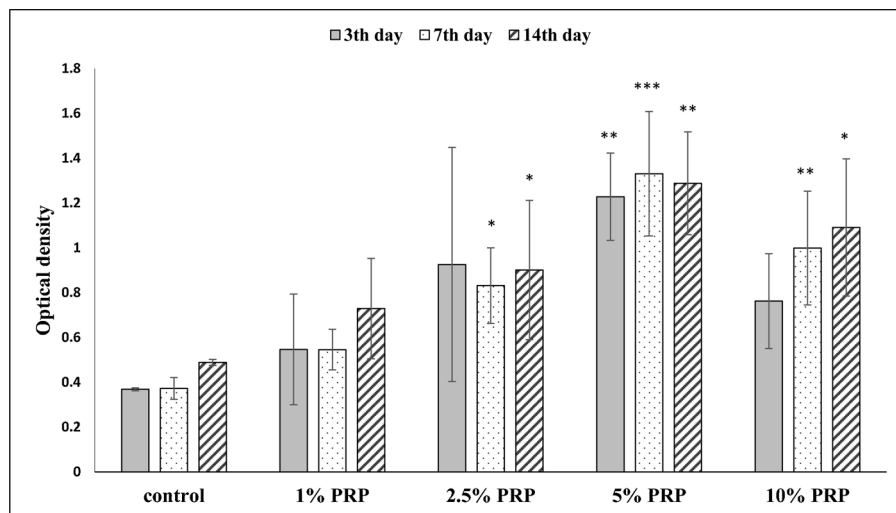


**Fig. 5.** SSCs cultured in culture medium with four different doses of PRP (1%, 2.5 %, 5%, and 10 %), MTT assay performed on third, seventh and fourteenth days to determine the optimized dose of PRP for cell viability and proliferation. The comparisons were carried out related to control group on each day, five samples were examined for each group and all evaluations were performed in five replications. Data expressed as means  $\pm$  SD (\*\*\*:  $p < 0.001$ ), (\*\*:  $p < 0.01$ ), (\*:  $p < 0.05$ ). As seen, the proliferation of SSCs in the culture medium including 5% PRP showed a significant increase in each day.

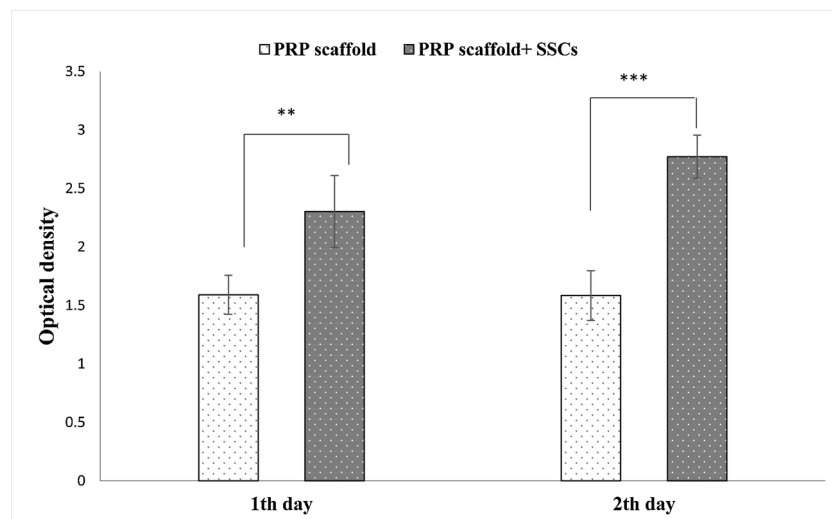


**Fig. 6.** MTT assay exhibited the cell viability on scaffolds at first and second days after cell seeding. Results presented as means  $\pm$  SD (\*\*\*:  $p < 0.001$ ), (\*\*:  $p < 0.01$ ), five samples were examined for each group and all evaluations were performed in five replications.

### 3.8. Gene expression evaluation by Real-time PCR in experimental groups

To confirm the existence of SSCs during the cell culture, the expression of GFRa1 and c-KIT evaluated in spermatogonial-cell-derived

colonies (Fig. 8). Our results showed that the expression of GFRa1 and c-KIT in the PRP- scaffold (3D) group significantly increased ( $p < 0.001$ ) as compared to the control group. In the PRP-2D group, the expression of GFRa1 showed no significant difference as compared to the control

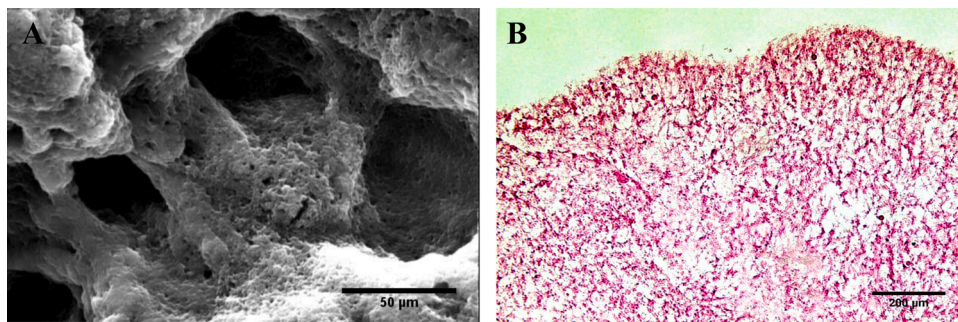


Fig. 7. Scaffold characterization.

A) SEM for determination of the biological and physical features related to the PRP-scaffold.  
 B) The mesh-like structure of PRP scaffold are seen in light microscopic image stained by H&E.

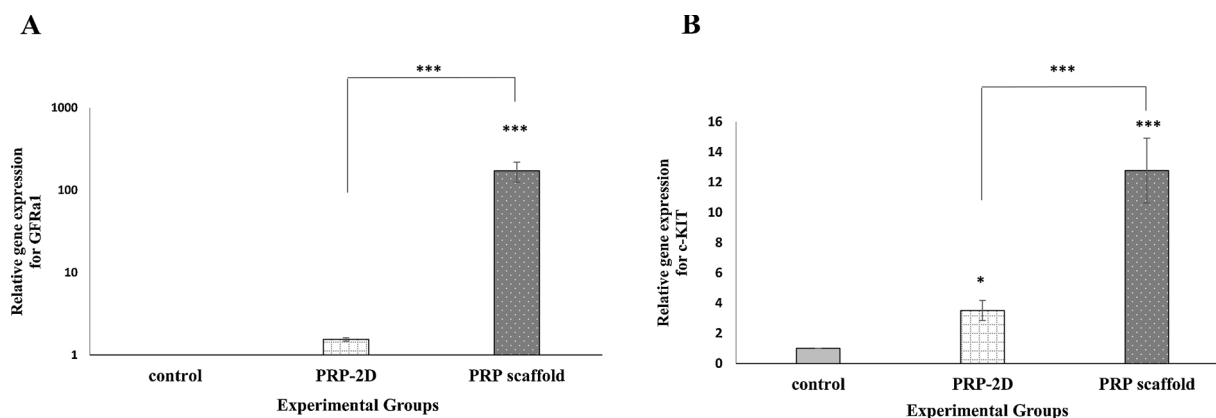


Fig. 8. The relative expression of GFRA1 and c-KIT genes of human SSCs derived from colonies developed in the PRP- 2D culture system and PRP- scaffold (3D group) analyzed by real-time PCR. Values are expressed as means  $\pm$  SD, five samples were examined for each group and all evaluations were performed in three replications. A: Expression of GFRA1 in the PRP scaffold group revealed a significant increase as compared with the control and PRP-2D groups (\*\*\*:  $p < 0.001$ ). B: Expression of c-KIT in the PRP scaffold group showed a significant increase as compared with other groups (\*\*\*:  $p < 0.001$ ). In PRP- 2D group, the expression of c-KIT had a significant increase as compared to the control group (\*:  $p < 0.05$ ).

group (Fig. 8A). The expression of c-KIT in the PRP-2D group significantly increased ( $p < 0.05$ ) as compared to the control group (Fig. 8B). Accordance with these findings, PRP has a remarkable outcome on the relative expression of genes involved in the proliferation and differentiation of SSCs.

### 3.9. Cell proliferation and cluster assay in different groups

Phenotypic and morphological characteristics of cells derived from human SSCs colonies are seen (Fig. 9). Colonies of human SSCs evaluated by an inverted microscope for the control and PRP-2D groups and SEM for the PRP scaffold group. As shown, Sertoli cells proliferated and

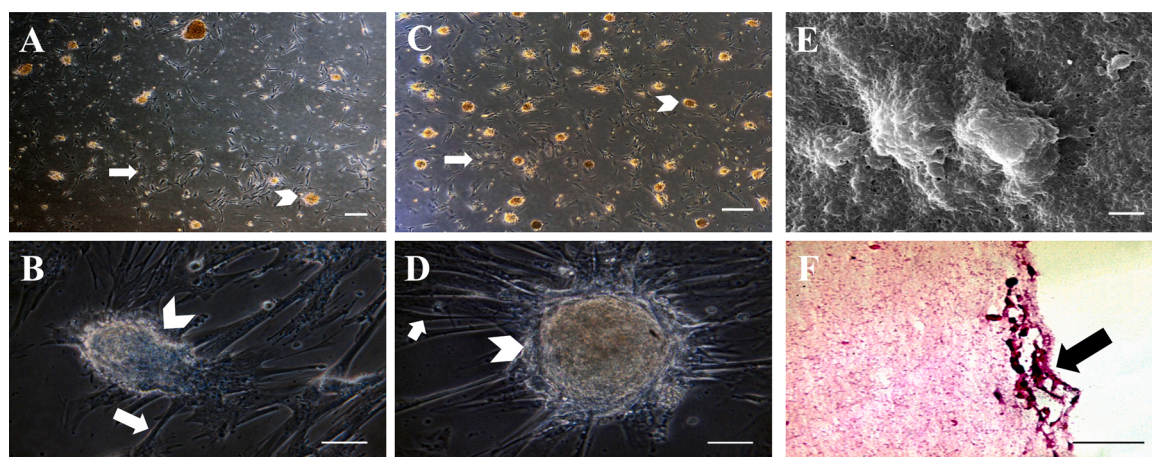


Fig. 9. Microscopic morphology of human SSCs in experimental groups at the end of the fourth week. A, B) Images obtained from control group C, D) Images taken from PRP- 2D group by inverted microscope, left arrows displayed the Sertoli cells and right arrows showed the colonies of SSCs made on top of Sertoli cells. E) SEM image displayed the colonies of human SSCs on the PRP scaffold. F) The light microscopic image exhibited the section of the SSCs on the PRP scaffold after the first week stained by H&E, arrow indicated the SSCs colony (scale bar for A, C=300  $\mu$ m, B, D, E, F = 50  $\mu$ m).

made a cell layer at the bottom of culture plate as a feeder surface; while SSCs created eminent colonies on Sertoli cells.

For evaluating the cell viability and proliferation of SSCs, we applied MTT assay at different groups (Fig. 10). Following the cell culture for 4 weeks, the result showed higher viability of SSCs on the PRP scaffold group in comparison to the control group (\*\*\*:  $p < 0.001$ ). Cell viability in PRP- 2D group also indicated a significant increase compared to the control group (\*\*\*:  $p < 0.001$ ), but not as much as the PRP scaffold group and a significant difference was observed between PRP scaffold and PRP-2D groups (\*\*\*:  $p < 0.001$ ). The number and diameter of colonies in the PRP-2D group increased significantly ( $p < 0.01$ ) as compared to the control group. Interestingly, in the PRP- scaffold group only the mean number of colonies increased significantly ( $p < 0.01$ ) related to the control group (Table 2).

#### 4. Discussion

In vitro proliferation of human SSCs remains a basic challenge in fertility preservation for pre-pubertal boys who were exposed to gonadotoxic therapies and non-obstructive azoospermia men. SSCs are scarce in the seminiferous tubules, thus a tiny portion of immature testicular biopsy includes a restricted percent of SSCs that by themselves are not sufficient for repopulation of a total testicular tissue after gonadotoxic treatment (Oatley and Brinster, 2008). The in vitro proliferation of SSCs before their autotransplantation is useful to achieve the whole repopulation of a mature testis. In present study, we assessed the adult human SSCs propagation instead of prepubertal testicular cells. According to previous researches, in vitro proliferation of SSCs from prepubertal animals such as rat, mouse, hamster and bovine successfully performed in culture systems similar to that described in our study (Aponte et al., 2008; Kanatsu-Shinohara et al., 2008, 2005). For the first time, we evaluated the effect of PRP on proliferation of human SSCs. Endogenous growth factors of platelets can release from the PRP scaffold, without cytokine delivery technologies or gene modifications. The randomly oriented fibrils organization in the PRP scaffold produced a conductive 3D culture system and contact guidance direction that increased cell proliferation and migration. (Xie et al., 2012). Similar to the findings of previous researches, the results of trypan blue staining in our study showed high viability (more than 80 %) rate of SSCs after two steps of enzymatic digestion (Izadyar et al., 2011; Mirzapour et al., 2015). This finding confirmed that the SSCs isolation method through the enzymatic digestion is a suitable and safe process. Cell suspension obtained from

**Table 2**

Comparison of colony numbers and diameters between control and experimental groups, Data are expressed as the mean and standard deviation from three independent measurements, five samples were considered for each group.

Groups	Colony numbers	Colony diameters
Control	16.25± 1.96	129.52± 30.85
PRP-2D	20± 2.28 <sup>a,b</sup>	158.53± 36.85 <sup>a,b</sup>
PRP-scaffold	23.5± 4.81 <sup>a</sup>	128.52± 27.44

<sup>a</sup> Significance difference as compared to the control group ( $p < 0.01$ ).

<sup>b</sup> Significance difference as compared to the PRP scaffold group ( $p < 0.01$ ).

two steps of enzymatic digestion included different spermatogenic cells at various stages of spermatogenesis as well as somatic cells. Similar to previous examinations (Jabari et al., 2020; Kokkinaki et al., 2011; Langenstroth et al., 2014), we used differential plating as SSCs enrichment method to decrease the number of somatic cells. Unlike our study, other previous investigations used MACS in order to the enrichment of human and mouse SSCs (Guo et al., 2015; Kanatsu-Shinohara et al., 2011; Kokkinaki et al., 2011). To eliminate most of the meiotic cells, post-meiotic cells and sperm from isolated cells obtained after enzymatic digestion, the cellular suspension cultivated for 3 weeks in proliferation basic medium. Basic culture medium including DMEM/F-12, GDNF, bFGF, LIF, FBS and KSR applied for 2D pre-culture and proliferation of testicular cells. Results of the previous studies showed KSR facilitated cell cycle progression and increased SSCs proliferation (Kubota et al., 2004b). Some of the other well-known growth factors needed for self-renewal and proliferation of SSCs are GDNF and GDNF family receptor  $\alpha 1$  (GFRa1), GFRa1 and Ret tyrosine kinase are the effective receptors for GDNF, the expression of GFRa1, Ret and Src family was seen in SSCs. GDNF through the GFRa1 activates Ret and kinases from the Src family. Consequently, activation of PI3K/Akt signaling pathway and expression of N-myc stimulates the proliferation of SSCs (Hofmann, 2008). bFGF is a crucial factor secreted from Sertoli cells and stimulates in vitro expansion and proliferation of SSCs, LIF act as an essential cytokine to in vitro propagation of SSCs, inhibit the apoptosis and promote the long-term culture of germ cells (Kubota et al., 2004a).

The purification rate of SSCs evaluated by flow cytometrical analysis using the PLZF marker, results of flow cytometry after 2D pre-culture reported a significant increase at the purification rate of SSCs in comparison with after two steps of enzymatic digestion. In agreement with our findings, other in vitro studies on human (Jabari et al., 2020), mice

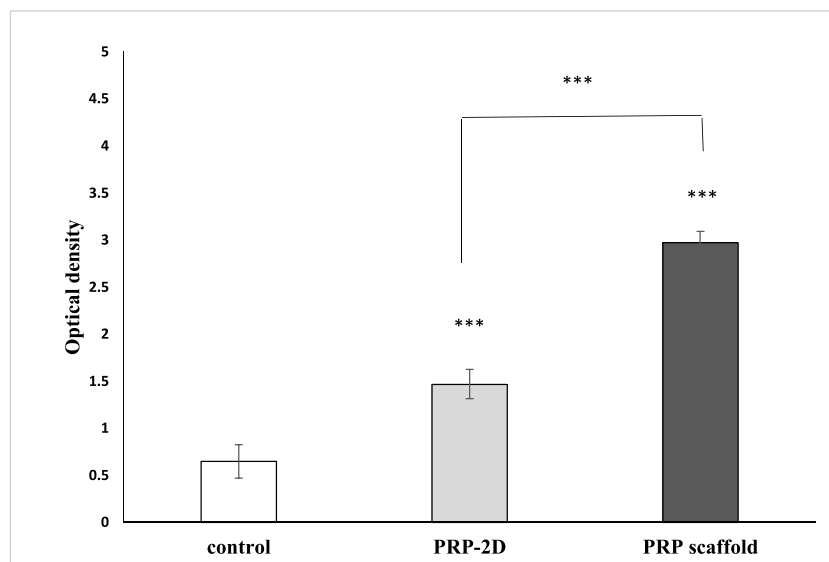


**Fig. 10.** MTT analysis for assessment of SSCs viability in various experimental groups at the end of fourth week. Data expressed means ± SD; (\*\*\*:  $p < 0.001$ ), five samples were examined for each group and all evaluations were performed in five replications.

(Azizollahi et al., 2016) and bovine SSCs (Izadyar et al., 2002) reported the efficient basic culture medium made a gradual increase in the purity rate of SSCs.

Results of RT-PCR displayed after 2D pre-culture of SSCs for 3 weeks, a significant increase in expression of pre-meiotic genes observed compared to after two steps of enzymatic digestion. Our findings were consistent with results of previous studies reported all of the pre-meiotic, meiotic and post-meiotic genes were expressed in cell suspension obtained after two steps of enzymatic digestion, whereas the expression of pre-meiotic genes significantly increased after 2D pre-culture of SSCs (Mirzapour et al., 2015; Mohammadzadeh et al., 2019). Previous publications have shown there are no distinct biochemical markers for SSCs (Brinster, 2002; McLean, 2008). For this reason, the expression of multiple markers such as spermatogonial and germ cell markers were evaluated. PLZF is a familial spermatogonial-specific marker in very species (Hermann et al., 2010), a general marker for stem cells is OCT4 (Ohmura et al., 2004), VASA as a marker of germ cells expressed in spermatogenic cells and the expression of Vimentin confirmed the presence of Sertoli cells in testicular tissue because it is the known intermediate filament in Sertoli cells (Ohbo et al., 2003).

Another human SSCs identification also performed through immunostaining, our results demonstrated colonies obtained after 2D pre-culture considerably revealed the expression of PLZF and GFRA1. In agreement with our study, previous investigations reported the expression of mice and human SSCs specific markers ( $\alpha 6$ -Integrin, PLZF, GFRA1, GPR125, UCHL1 and THY1) on colony derived from 2D pre-culture of SSCs (Gholami et al., 2018; Guo et al., 2015; Navid et al., 2017). In a previous study (Mohammadzadeh et al., 2019) to confirm the absence of meiotic proteins after 2D pre-culture, the expression of SCP3, Acrosin and Stra8 genes evaluated by real-time PCR and results reported that expression of the meiotic markers was not observed 3 weeks after culture. Moreover, other previous investigations by Immunocytochemistry revealed the expression of SCP3 (meiotic protein) and PROTAMINE 1 (post-meiotic protein) was not seen in SSCs colonies after 2D pre-culture of cells (Gholami et al., 2018; Jabari et al., 2020).

There are various markers (ITGA6, GPR125, GFRA1, UCHL1 and PLZF) to distinguish human SSCs. Since these markers can also be recognized in several testicular somatic cells, recommending that they are not dependable. To determine whether cultured human spermatogonial cells are really functional germ cells, the only reliable evaluation is the transplantation of in vitro-cultured SSCs into a recipient testis. In this examination, SSCs functional assay of the cluster cells was also done by xenotransplantation to azoospermia model, in addition to confirmation of molecular characteristics. There are no distinct morphological markers for SSCs and they are the only cells that able to recolonize in the infertile animals seminiferous tubules (Shinohara et al., 2000). 2D pre cultured testicular cells transplanted into the efferent ducts of busulfan azoospermia mouse, to confirm the functionality of SSCs in our culture system after 3 weeks. Finally, colonization and homing of SSCs in recipient mouse testes evaluated through a fluorescent microscope. Similar to findings of previous studies, SSCs observed on the basement membrane of the cross-sectioned tubules (Nagano et al., 1999; Nick-kholgh et al., 2014). The present investigation demonstrated that human SSCs after proliferation are entirely functional, and the culturing process does not impair the surface characteristics of them

Since there was no study to evaluate the effect of PRP on the proliferation of SSCs, we cultured SSCs by 4 different doses of PRP for 2 weeks and used MTT assay to determine the optimum dose of PRP. When we applied PRP10 %, we observed the generation of dense and sharp-edged colonies named ES-like cells colonies. Previous studies suggested in vitro culture conditions for the proliferation of adult human SSCs may lead to the formation of ES-like colonies. Multipotency characteristics and multilineage differentiation of human SSCs under in vivo environments were probably prohibited. While, in vitro culture of SSCs maybe lead to eliminating this prohibition and formation of pluripotent stem cells (Golestaneh et al., 2009; Mizrak et al., 2010).

As seen above, 2D and 3D culture systems of PRP could significantly increase in vitro colony formation, which may be due to the proper cell to cell and cells to ECM like scaffold interaction (Woo et al., 2007). Results of our study revealed the number and diameter of colonies in the PRP-2D group significantly increased as compared to the control group, while in the PRP scaffold group a significant increase observed only in the number of colonies. Similar to our findings, another previous investigation on human SSCs displayed the number of SSCs colonies significantly increased in soft agar culture system compared to gelatin-coated plates, whereas the diameter of colonies showed no significant difference (Mohammadzadeh et al., 2019). Since the number of colonies was more abundant in the PRP scaffold group, this illustrates why the diameter of colonies diminished after SSCs cultivation on the PRP scaffold. It would be possible that diameter of colonies significantly increase in long term culture of SSCs. In contrast, Gholami et al. (2018) reported the number and diameter of colonies significantly increased in soft agar culture system as compared to control group. The liquid PRP used in a 2D culture system can be blended with SSCs before it was activated by  $\text{CaCl}_2$  and create the fibrin clot. Based on these findings the significant difference between the results of PRP-2D and PRP scaffold groups is defensible (Kang et al., 2011).

The relative expression of GFRA1 and c-KIT (involved in maintaining undifferentiated state and progression to differentiated state, respectively) assessed by real-time PCR. As mentioned the relative expression of these genes in the PRP scaffold group revealed a significant increase as compared to other groups. Previous investigations have determined the impacts of different growth factors from the platelets on various cellular events. PDGF, EGF, bFGF, IGF-1 stimulated cell proliferation, FGF and IGF-1 also regulated cell differentiation (Salamanna et al., 2015). Platelets growth factors not only have their specific effects but also by interacting with other growth factors, stimulated the activation of gene expression and protein production

(Vaquero et al., 2013). bFGF leads to the generation of GFRA1 and GDNF, this factor acted in an autocrine state and leading to a reduction in cells apoptotic signaling (Lenhard et al., 2002). By adding IGF-1 to the SSCs culture medium the proliferation of cells increased after 6 weeks, this finding suggested that SSCs can be modulated by IGF-1. IGF-1 activated the PI3K/Akt and mitogen-activated protein kinase pathways that stimulated cell proliferation and cell survival (LeRoith and Roberts, 2003), this pathway may interact with the GDNF signaling and likely promote self-renewal and proliferation of SSCs. In order to long-term cultures of SSCs, GDNF and FGF2 are well-known growth factors utilized recently. According to results of the previous study, FGF2 and GDNF through activation of PI3K/AKT and MAPK signaling pathway lead to enhancement in the number and proliferation of SSCs (Kubota et al., 2004b). Previous experiments recommended that responsibility of SSCs to FGF2 enhanced when GDNF used. On the other hand, GDNF stimulated the expression of fibroblast growth factor receptor-2 (FGFR2) and we concluded that GDNF could enhance indirectly the effects of platelet growth factor (Hofmann, 2008; Hofmann et al., 2005). Other growth factors of PRP such as EGF and PDGF increased the expression of genes involved in proliferation and differentiation of cells by activation in ERK signaling pathway (Stevens and Khetarpal, 2019).

SEM observations demonstrated that SSCs attached to a solid scaffold, recommending cells could be motivated efficiently without extra migration. These capabilities could be very valuable in the proliferation of SSCs and clonal expansion. In agreement with the previous studies, our histological findings also revealed the PRP scaffold act as a potential cell carrier, because of its 3-D mesh-like structure. (Liou et al., 2018; Tajima et al., 2015). Due to the presence of numerous hydrophilic groups, the PRP scaffold as a hydrogel has great water content. Great water content in this 3D culture system promotes the delivery of nutrients and transfer of waste compositions (Jana et al., 2014). Low mechanical strength and rapid degradation characteristics of PRP scaffold can also be associated to the high water content of this hydrogel (Ahearne et al., 2008). Unlike the soft agar culture system, it isn't

possible to observe and evaluate SSCs colonies by inverted microscope, only micrographs obtained from SEM could provide information around the proliferation and colonization of human SSCs and this is one of the most major limitations of the PRP scaffold.

## 5. Conclusions

Besides the limitations of this research, we have realized PRP is a simply accessible blood derivative including high concentrations of growth factors. We have demonstrated the optimal concentration of PRP plays a principal role in promoting the in vitro 2D proliferation of SSCs. Besides, our findings indicated the activation of PRP by CaCl<sub>2</sub> and formation of PRP scaffold as a 3D structure increased propagation of SSCs remarkably. The potential of these platelet-rich preparations is mainly due to the cytokines, growth factors obtained from platelets and 3D microstructure of PRP scaffold that mimic the niche of SSCs. These findings provided convincing proof and useful data for the application of PRP to infertility treatment and suggested that future clinical studies should be done to understand PRP mechanisms that affect clinical outcomes.

## CRedit authorship contribution statement

**Farnaz Khadivi:** Writing - original draft, Data curation, Conceptualization. **Morteza Koruji:** Methodology, Project administration, Writing - review & editing, Formal analysis, Visualization. **Mohammad Akbari:** Validation, Resources. **Ayob Jabari:** Data curation, Investigation. **Ali Talebi:** Investigation, Resources. **Sepideh Ashouri Movasagh:** Software, Formal analysis. **Amin Panahi Boroujeni:** Validation, Data curation. **Narjes Feizollahi:** Software. **Aghbib Nikmahzar:** Formal analysis. **Mohammad Pourahmadi:** Resources, Data curation. **Mehdi Abbasi:** Supervision, Project administration, Funding acquisition.

## Declaration of Competing Interest

The authors declare that there is no conflict of interest.

## Acknowledgments

The present work was supported by a grant (No. 39672) from the Tehran University of Medical Sciences. The results of this article were a part of a Ph.D. student thesis.

## References

- Ahearne, M., Yang, Y., Liu, K., 2008. Mechanical characterisation of hydrogels for tissue engineering applications. *Topics Tissue Eng.* 4 (12), 1–16.
- Aponte, P.M., Soda, T., Teerds, K.J., Mizrak, S.C., van de Kant, H.J., de Rooij, D.G., 2008. Propagation of bovine spermatogonial stem cells in vitro. *Reproduction* 136 (5), 543–557.
- Azizollahi, S., Afatoonian, R., Gilani, M.A.S., Behnam, B., Tajik, N., Asghari-Jafarabadi, M., Asgari, H.R., Koruji, M., 2016. Alteration of spermatogenesis following spermatogonial stem cells transplantation in testicular torsion-detorsion mice. *J. Assist. Reprod. Genet.* 33 (6), 771–781.
- Basciani, S., Mariani, S., Arizzi, M., Ulisse, S., Rucci, N., Jannini, E.A., Rocca, C.D., Manicone, A., Carani, C., Spera, G., 2002. Expression of platelet-derived growth factor-A (PDGF-A), PDGF-B, and PDGF receptor- $\alpha$  and - $\beta$  during human testicular development and disease. *J. Clin. Endocrinol. Metab.* 87 (5), 2310–2319.
- Brinster, R.L., 2002. Germline stem cell transplantation and transgenesis. *Science* 296 (5576), 2174–2176.
- Chu, C., Schmidt, J.J., Carnes, K., Zhang, Z., Kong, H.J., Hofmann, M.-C., 2009. Three-dimensional synthetic niche components to control germ cell proliferation. *Tissue Eng. Part A* 15 (2), 255–262.
- Elhija, M.A., Lunenfeld, E., Schlatt, S., Huleihel, M., 2012. Differentiation of murine male germ cells to spermatozoa in a soft agar culture system. *Asian J. Androl.* 14 (2), 285.
- Eom, Y.W., Oh, J.-E., Lee, J.L., Baik, S.K., Rhee, K.-J., Shin, H.C., Kim, Y.M., Ahn, C.M., Kong, J.H., Kim, H.S., 2014. The role of growth factors in maintenance of stemness in bone marrow-derived mesenchymal stem cells. *Biochem. Biophys. Res. Commun.* 445 (1), 16–22.
- Fayomi, A.P., Orwig, K.E., 2018. Spermatogonial stem cells and spermatogenesis in mice, monkeys and men. *Stem Cell Res.* 29, 207–214.
- Gholami, K., Pourmand, G., Koruji, M., Sadighilani, M., Navid, S., Izadyar, F., Abbasi, M., 2018. Efficiency of colony formation and differentiation of human spermatogenic cells in two different culture systems. *Reprod. Biol.* 18 (4), 397–403.
- Golestaneh, N., Kokkinaki, M., Pant, D., Jiang, J., DeStefano, D., Fernandez-Bueno, C., Rone, J.D., Haddad, B.R., Gallicano, G.I., Dym, M., 2009. Pluripotent stem cells derived from adult human testes. *Stem Cells Dev.* 18 (8), 1115–1125.
- Guo, Y., Liu, L., Sun, M., Hai, Y., Li, Z., He, Z., 2015. Expansion and long-term culture of human spermatogonial stem cells via the activation of SMAD3 and AKT pathways. *Exp. Biol. Med.* 240 (8), 1112–1122.
- Hermann, B.P., Sukhwani, M., Hansel, M.C., Orwig, K.E., 2010. Spermatogonial stem cells in higher primates: are there differences to those in rodents? *Reproduction (Cambridge Engl.)* 139 (3), 479.
- Hofmann, M.-C., 2008. Gdnf signaling pathways within the mammalian spermatogonial stem cell niche. *Mol. Cell. Endocrinol.* 288 (1–2), 95–103.
- Hofmann, M.-C., Braydich-Stolle, L., Dym, M., 2005. Isolation of male germ-line stem cells; influence of GDNF. *Dev. Biol.* 279 (1), 114–124.
- Huleihel, M., Nourashrafeddin, S., Plant, T.M., 2015. Application of three-dimensional culture systems to study mammalian spermatogenesis, with an emphasis on the rhesus monkey (*Macaca mulatta*). *Asian J. Androl.* 17 (6), 972.
- Izadyar, F., Spierenberg, G., Creemers, L., Ouden, Kd., De Rooij, D., 2002. Isolation and purification of type A spermatogonia from the bovine testis. *Reproduction* 124 (1), 85–94.
- Izadyar, F., Wong, J., Maki, C., Pacchiarotti, J., Ramos, T., Howerton, K., Yuen, C., Greilach, S., Zhao, H.H., Chow, M., 2011. Identification and characterization of repopulating spermatogonial stem cells from the adult human testis. *Hum. Reprod.* 26 (6), 1296–1306.
- Jabari, A., Gilani, M.A.S., Koruji, M., Gholami, K., Mohsenzadeh, M., Khadivi, F., Gashfi, N.G., Nikmahzar, A., Mojaverrostami, S., Talebi, A., 2020. Three-dimensional co-culture of human spermatogonial stem cells with Sertoli cells in soft agar culture system supplemented by growth factors and Laminin. *Acta Histochem.* 122 (5), 151572.
- Jana, S., Banerjee, A., Gandhi, A., 2014. Preparation and characterization of chitosan based polyelectrolyte complex as a carrier of aceclofenac. *J. PharmaSciTech.* 3 (2), 1–4.
- Kanatsu-Shinohara, M., Ogonuki, N., Iwano, T., Lee, J., Kazuki, Y., Inoue, K., Miki, H., Takehashi, M., Toyokuni, S., Shinkai, Y., 2005. Genetic and epigenetic properties of mouse male germline stem cells during long-term culture. *Development* 132 (18), 4155–4163.
- Kanatsu-Shinohara, M., Muneto, T., Lee, J., Takenaka, M., Chuma, S., Nakatsuji, N., Horiuchi, T., Shinohara, T., 2008. Long-term culture of male germline stem cells from hamster testes. *Biol. Reprod.* 78 (4), 611–617.
- Kanatsu-Shinohara, M., Inoue, K., Ogonuki, N., Morimoto, H., Ogura, A., Shinohara, T., 2011. Serum- and feeder-free culture of mouse germline stem cells. *Biol. Reprod.* 84 (1), 97–105.
- Kang, Y.-H., Jeon, S.H., Park, J.-Y., Chung, J.-H., Choung, Y.-H., Choung, H.-W., Kim, E.-S., Choung, P.-H., 2011. Platelet-rich fibrin is a Bioscaffold and reservoir of growth factors for tissue regeneration. *Tissue Eng. Part A* 17 (3–4), 349–359.
- Khadivi, F., Razavi, S., Hashemi, F., 2020. Protective effects of zinc on rat sperm chromatin integrity involvement: DNA methylation, DNA fragmentation, ubiquitination and protamination after bleomycin etoposide and cis-platin treatment. *Theriogenology* 142, 177–183.
- Kokkinaki, M., Djourabtchi, A., Golestaneh, N., 2011. Long-term culture of human SSEA-4 positive spermatogonial stem cells (SSCs). *J. Stem Cell Res. Ther. (Edmond)* 2 (2), 2488.
- Kostereva, N., Hofmann, M.C., 2008. Regulation of the spermatogonial stem cell niche. *Reprod. Domest. Anim.* 43, 386–392.
- Kubota, H., Brinster, R.L., 2018. Spermatogonial stem cells. *Biol. Reprod.* 99 (1), 52–74.
- Kubota, H., Avarbock, M.R., Brinster, R.L., 2004a. Culture conditions and single growth factors affect fate determination of mouse spermatogonial stem cells. *Biol. Reprod.* 71 (3), 722–731.
- Kubota, H., Avarbock, M.R., Brinster, R.L., 2004b. Growth factors essential for self-renewal and expansion of mouse spermatogonial stem cells. *Proc. Natl. Acad. Sci. U. S. A.* 101 (47), 16489–16494.
- Langenstroth, D., Kossack, N., Westernströer, B., Wistuba, J., Behr, R., Gromoll, J., Schlatt, S., 2014. Separation of somatic and germ cells is required to establish primate spermatogonial cultures. *Hum. Reprod.* 29 (9), 2018–2031.
- Lee, J.H., Kim, H.J., Kim, H., Lee, S.J., Gye, M.C., 2006. In vitro spermatogenesis by three-dimensional culture of rat testicular cells in collagen gel matrix. *Biomaterials* 27 (14), 2845–2853.
- Lenhard, T., Schober, A., Suter-Crazzolaro, C., Unsicker, K., 2002. Fibroblast growth factor-2 requires glial-cell-line-derived neurotrophic factor for exerting its neuroprotective actions on glutamate-lesioned hippocampal neurons. *Mol. Cell. Neurosci.* 20 (2), 181–197.
- LeRoith, D., Roberts Jr, C.T., 2003. The insulin-like growth factor system and cancer. *Cancer Lett.* 195 (2), 127–137.
- Li, Y., Higashi, Y., Itabe, H., Song, Y.-H., Du, J., Delafontaine, P., 2003. Insulin-like growth factor-1 receptor activation inhibits oxidized LDL-induced cytochrome C release and apoptosis via the phosphatidylinositol 3 kinase/Akt signaling pathway. *Arterioscler. Thromb. Vasc. Biol.* 23 (12), 2178–2184.
- Liou, J.-J., Rothrauff, B.B., Alexander, P.G., Tuan, R.S., 2018. Effect of platelet-rich plasma on chondrogenic differentiation of adipose- and bone marrow-derived mesenchymal stem cells. *Tissue Eng. Part A* 24 (19–20), 1432–1443.
- McLean, D.J., 2008. Spermatogonial stem cell transplantation, testicular function, and restoration of male fertility in mice. *Methods Mol. Biol.* 450, 149–162.
- Mei-Dan, O., Laver, L., Nyska, M., Mann, G., 2011. Platelet rich plasma—a new biotechnology for treatment of sports injuries. *Harefuah* 150 (5), 453–457, 490.

- Mirzapour, T., Movahedin, M., Koruji, M., Nowroozi, M., 2015. Xenotransplantation assessment: morphometric study of human spermatogonial stem cells in recipient mouse testes. *Andrologia* 47 (6), 626–633.
- Mirzapour, T., Tengku Ibrahim, T., Movahedin, M., Nowroozi, M., 2017. Morphological and ultrastructural studies of human spermatogonial stem cells from patients with maturation arrest. *Andrologia* 49 (7), e12700.
- Mizrak, S., Chikhovskaya, J., Sadri-Ardekani, H., Van Daalen, S., Korver, C., Hovingh, S., Roepers-Gajadien, H., Raya, A., Fluiter, K., de Reijke, T.M., 2010. Embryonic stem cell-like cells derived from adult human testis. *Hum. Reprod.* 25 (1), 158–167.
- Mohammadzadeh, E., Mirzapour, T., Nowroozi, M.R., Nazarian, H., Piryaei, A., Alipour, F., Modarres Mousavi, S.M., Ghaffari Novin, M., 2019. Differentiation of spermatogonial stem cells by soft agar three-dimensional culture system. *Artif. Cells Nanomed. Biotechnol.* 47 (1), 1772–1781.
- Nagano, M., Avarbock, M.R., Brinster, R.L., 1999. Pattern and kinetics of mouse donor spermatogonial stem cell colonization in recipient testes. *Biol. Reprod.* 60 (6), 1429–1436.
- Nakamura, B.N., Lawson, G., Chan, J.Y., Banuelos, J., Cortés, M.M., Hoang, Y.D., Ortiz, L., Rau, B.A., Luderer, U., 2010. Knockout of the transcription factor NRF2 disrupts spermatogenesis in an age-dependent manner. *Free Radic. Biol. Med.* 49 (9), 1368–1379.
- Navid, S., Rastegar, T., Baazm, M., Alizadeh, R., Talebi, A., Gholami, K., Khosravi-Farsani, S., Koruji, M., Abbasi, M., 2017. In vitro effects of melatonin on colonization of neonate mouse spermatogonial stem cells. *Syst. Biol. Reprod. Med.* 63 (6), 370–381.
- Nickkholgh, B., Mizrak, S.C., Korver, C.M., van Daalen, S.K., Meissner, A., Repping, S., van Pelt, A.M., 2014. Enrichment of spermatogonial stem cells from long-term cultured human testicular cells. *Fertil. Steril.* 102 (2), 558–565 e555.
- Oatley, J.M., Brinster, R.L., 2008. Regulation of spermatogonial stem cell self-renewal in mammals. *Annu. Rev. Cell Dev. Biol.* 24, 263–286.
- Ohbo, K., Yoshida, S., Ohmura, M., Ohneda, O., Ogawa, T., Tsuchiya, H., Kuwana, T., Kehler, J., Abe, K., Schöler, H.R., 2003. Identification and characterization of stem cells in prepubertal spermatogenesis in mice. *Dev. Biol.* 258 (1), 209–225.
- Ohmura, M., Yoshida, S., Ide, Y., Nagamatsu, G., Suda, T., Ohbo, K., 2004. Spatial analysis of germ stem cell development in Oct-4/EGFP transgenic mice. *Arch. Histol. Cytol.* 67 (4), 285–296.
- Romerius, P., Ståhl, O., Moëll, C., Relander, T., Cavallin-Ståhl, E., Wiebe, T., Giwercman, Y., Giwercman, A., 2011. High risk of azoospermia in men treated for childhood cancer. *Int. J. Androl.* 34 (1), 69–76.
- Salamanna, F., Veronesi, F., Maglio, M., Della Bella, E., Sartori, M., Fini, M., 2015. New and emerging strategies in platelet-rich plasma application in musculoskeletal regenerative procedures: general overview on still open questions and outlook. *Biomed. Res. Int.* 2015.
- Schindelin, J., Rueden, C., Hiner, M., Eliceiri, K., 2015. The ImageJ ecosystem: an open platform for biomedical image analysis. *Mol. Reprod. Dev.* 82, 518–529.
- Sharkey, D.J., Tremellen, K.P., Briggs, N.E., Dekker, G.A., Robertson, S.A., 2016. Seminal plasma transforming growth factor- $\beta$ , activin A and follistatin fluctuate within men over time. *Hum. Reprod.* 31 (10), 2183–2191.
- Shinohara, T., Orwig, K.E., Avarbock, M.R., Brinster, R.L., 2000. Spermatogonial stem cell enrichment by multiparameter selection of mouse testis cells. *Proc. Natl. Acad. Sci. U. S. A.* 97 (15), 8346–8351.
- Stevens, J., Khetarpal, S., 2019. Platelet-rich plasma for androgenetic alopecia: a review of the literature and proposed treatment protocol. *Int. J. Womens Dermatol.* 5 (1), 46–51.
- Stukenborg, J.-B., Schlatt, S., Simoni, M., Yeung, C.-H., Elhija, M.A., Luetjens, C.M., Huleihel, M., Wistuba, J., 2009. New horizons for in vitro spermatogenesis? An update on novel three-dimensional culture systems as tools for meiotic and post-meiotic differentiation of testicular germ cells. *Mol. Hum. Reprod.* 15 (9), 521–529.
- Susilowati, S., Triana, I.N., Malik, A., 2015. The effects of insulin-like growth factor I (IGF-I) complex from seminal plasma on capacitation, membrane integrity and DNA fragmentation in goat spermatozoa. *Asian Pac. J. Reprod.* 4 (3), 208–211.
- Tajima, S., Tobita, M., Orbay, H., Hyakusoku, H., Mizuno, H., 2015. Direct and indirect effects of a combination of adipose-derived stem cells and platelet-rich plasma on bone regeneration. *Tissue Eng. Part A* 21 (5–6), 895–905.
- Tobita, M., Tajima, S., Mizuno, H., 2015. Adipose tissue-derived mesenchymal stem cells and platelet-rich plasma: stem cell transplantation methods that enhance stemness. *Stem Cell Res. Ther.* 6 (1), 215.
- van Dorp, W., van Beek, R.D., Laven, J., Pieters, R., de Muinck Keizer-Schrama, S., Van den Heuvel-Eibrink, M., 2012. Long-term endocrine side effects of childhood Hodgkin's lymphoma treatment: a review. *Hum. Reprod. Update* 18 (1), 12–28.
- Vaquero, J., Otero, L., Bonilla, C., Aguayo, C., Rico, M.A., Rodríguez, A., Zurita, M., 2013. Cell therapy with bone marrow stromal cells after intracerebral hemorrhage: impact of platelet-rich plasma scaffolds. *Cytotherapy* 15 (1), 33–43.
- Ward, E., DeSantis, C., Robbins, A., Kohler, B., Jemal, A., 2014. Childhood and adolescent cancer statistics, 2014. *CA Cancer J. Clin.* 64 (2), 83–103.
- Woo, K.M., Jun, J.-H., Chen, V.J., Seo, J., Baek, J.-H., Ryoo, H.-M., Kim, G.-S., Somerman, M.J., Ma, P.X., 2007. Nano-fibrous scaffolding promotes osteoblast differentiation and biomineralization. *Biomaterials* 28 (2), 335–343.
- Xie, X., Wang, Y., Zhao, C., Guo, S., Liu, S., Jia, W., Tuan, R.S., Zhang, C., 2012. Comparative evaluation of MSCs from bone marrow and adipose tissue seeded in PRP-derived scaffold for cartilage regeneration. *Biomaterials* 33 (29), 7008–7018.